

An infinite family of $bc8$ -like metastable phases in silicon

Vladimir E. Dmitrienko* and Viacheslav A. Chizhikov†
*A.V. Shubnikov Institute of Crystallography, FSRC “Crystallography
and Photonics” RAS, Leninskiy Prospekt 59, 119333, Moscow, Russia*

We show that new silicon crystalline phases, observed in the experiment with the laser-induced microexplosions inside silicon crystals (Rapp *et al.* Nat. Commun. **6**, 7555 (2015)), are all superstructures of a disordered high-symmetry phase with $Ia\bar{3}d$ cubic space group, as well as known for many years phases $bc8$ (Si-III) and $r8$ (Si-XII). The physics of this phenomenon is rather nontrivial: The $bc8$ -like superstructures appear as regularly ordered patterns of switchable atomic strings, preserving everywhere the energetically favorable tetrahedral coordination of silicon atoms. The variety of superstructures arises because each string can be switched between two states independently of the others. An infinite family of different phases can be obtained this way and a number of them are considered here in detail. In addition to the known $bc8$, $bt8$, and $r8$ crystals, 128 tetrahedral structures with 16 (6 phases), 24 (22 phases), and 32 (100 phases) atoms per primitive cell are generated and studied, most of them are new ones. For the coarse-grain description of the structures with two possible states of switchable strings, the black/white (switched/nonswitched) Shubnikov symmetry groups has been used. An *ab initio* relaxation of the atomic positions and lattice parameters shows that all the considered phases are metastable and have higher density and energy relative to the $bc8$ phase at the ambient pressure. A possible scenario for appearance of those phases from the high-temperature amorphous phase is discussed.

PACS numbers:

INTRODUCTION

Despite the fact that our contemporary civilization is now based on one type of silicon crystals with the diamond structure, this chemical element is not much inferior to carbon in the diversity of its allotropes. There are numerous exotic structures with tetrahedral [1, 2] and more complicated atomic arrangements, including a big family of high-pressure silicon phases with higher coordinations [3–5]. The silicon phases are interesting first of all owing to their electronic properties and the latter are determined by details of the atomic structures and impurities. Another promising application is related to micro-electromechanical systems (MEMS) [6] where the elastic properties of silicon are used. For all these purposes, one needs to look for new silicon-based crystals with the hope to find new unusual properties and applications.

One of the exotic tetrahedral structures, the $bc8$ phase, had been discovered in 1963 [7, 8]; its name means body-centered cubic with 8 atoms per the primitive cell (that is 16 atoms per the bcc unit cell, the lattice parameter $a = 6.64$ Å, and the space group is $Ia\bar{3}$). It is also called Si-III because it had been found after Si-I (diamond-like) and Si-II (β -Sn-like) silicon phases [3, 4]. All the atoms in $bc8$ are crystallographically equivalent, they are located at the three-fold axes, ($16c$) sites x, x, x of the cubic cell ($x \approx 0.1$), and have non-ideal tetrahedral coordination

with one interatomic bond directed along a three-fold cubic axis (A -bond) and three longer bonds (B -bonds) in non-symmetric directions. Structurally, the $bc8$ phase can be considered as the cubic arrangement of atomic strings directed along four $\langle 111 \rangle$ axes (this point is discussed in detail below). The $bc8$ phase was first obtained from the high-pressure β -Sn-like phase after pressure release [7, 8] and was found to be metastable at the ambient conditions. Its structural and electronic properties have been studied in detail for many years [9–15]. In the $bc8$ phase, like in diamond, there are only even-membered rings of interatomic bonds and the minimal rings are six-membered.

The first $bc8$ -like structure, $r8$ or Si-XII, had been discovered in 1994 [16]; $r8$ means rhombohedral with 8 atoms per the unit cell, its space group is $R\bar{3}$, a subgroup of $Ia\bar{3}$. The $r8$ phase appears from $bc8$ in the first-order pressure-induced structural transition as a result of breaking and rebonding of all the A -bonds directed along the $[111]$ cubic direction. Indeed, according to [16], the rebonding can be understood as motion of the atom at (x, x, x) along the $[111]$ direction of the $bc8$ unit cell until the A -bond to the atom at $(\bar{x}, \bar{x}, \bar{x})$ is broken and a new A -bond to the atom at $(\frac{1}{2} - x, \frac{1}{2} - x, \frac{1}{2} - x)$ is formed (Fig. 1). As a result of the rebonding, all the $[111]$ atomic strings are switched into another sequence of bonds preserving nevertheless the energetically favorable tetrahedral atomic arrangement. The phase transition is of the first order because the rebonding is accompanied by small but finite atomic displacements changing the topology of rings, in particular, five-membered rings appear in the $r8$ phase.

Both $bc8$ and $r8$ phases can also appear as a result

*email: dmitrien@crys.ras.ru

†email: chizhikov@crys.ras.ru

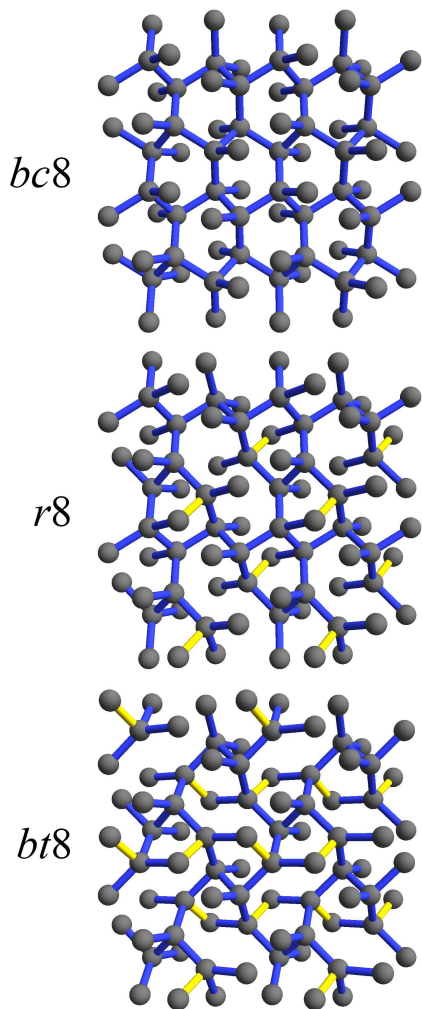


FIG. 1: (Color online) Comparison of the crystalline silicon structures *bc8*, *r8*, and *bt8*. An atomic layer is chosen to be parallel to the plane (100) of the *bc8* crystal. In the phases *r8* and *bt8*, the bonds coinciding with those of *bc8* are shown in blue, and the new switched bonds along the $\langle 111 \rangle$ directions are yellow.

of mechanical microindentation and their thermal relaxation back to the diamond silicon has been studied in numerous research works [17–20]. The electronic and optical properties of *bc8* and *r8* phases may have interesting practical applications (see [21, 22] and references therein).

In 1999, it was shown [23, 24] that the rebonding mechanism found by Crain *et al.* [16] is rather universal: in the *bc8* structure, any set of the atomic strings can be independently switched without violation of tetrahedral coordination. In particular, a new tetragonal silicon phase (*bt8*) was predicted, where all the strings of *bc8* parallel to two cubic diagonals (say $[111]$ and $[\bar{1}\bar{1}\bar{1}]$) were switched and those parallel to $[1\bar{1}\bar{1}]$ and $[\bar{1}1\bar{1}]$ were not (Fig. 1). The space symmetry of *bt8* is $I4_1/a$ and it is

not a subgroup of $Ia\bar{3}$: there are new symmetry elements, fourfold screw axes, relating switched and non-switched strings. The *bt8* phase demonstrates the maximum density of five-membered bond rings [24] and its electronic properties are expected to be rather different from those of *bc8*, *r8*, and diamond phases. Energetics and structural relaxation of *bt8* have been studied *ab initio* both for silicon [24] and carbon [25]. It has been shown that at the ambient pressure *bt8* is more dense than *bc8* and *r8* and it becomes energetically more favorable than *bc8* and *r8* at pressures above 13 GPa where the β -tin silicon structure is, in fact, more favorable than all the *bc8*-like phases. Later on, in 2013, the *bt8* structure was independently reinvented and studied *ab initio* for silicon and germanium [26] and for carbon [27] (in the latter case the symmetry was claimed to be $I4_1$ whereas the calculated atomic coordinates corresponded in fact to the more symmetric $I4_1/a$ space group). The *bc8*-like structures were also studied by the algebraic geometry [28] and by high-dimensional projection methods used for quasicrystals and their approximants [29].

The real breakthrough has happened in 2015 when Rapp *et al.* [30] have found evidence for several metastable silicon phases after ultrashort laser-induced confined microexplosions [31] at the interface between a transparent amorphous silicon dioxide layer (SiO_2) and an opaque single-crystal Si substrate. They have determined the lattice parameters and possible atomic structures of the following phases: *bt8*, *st12* (analog of *st12* in germanium), two tetragonal phases with 32 atoms per unit cells, and some others. For the description of the structures they used an *ab initio* random structure search [32]. It should be noted that one of the 32-atoms tetragonal phases was found independently [33] using the ideas of metadynamics and evolutionary algorithms. The exotic silicon phases like *bc8*, *r8*, and those new discovered by Rapp *et al.* [30] have provided a novel insight into the local structure and properties of the amorphous phase of silicon [9, 10, 23, 34].

In the present paper we suggest a unified description of all new silicon crystalline phases (except *st12*) observed by Rapp *et al.* [30] and numerous similar phases. Those complicated phases are shown to be the *bc8*-like structures with periodically switched strings, like in the simple case of *r8*. As a result, the lattice vectors of those phases are some periods of *bc8*. In addition to known *bc8*, *r8*, and *bt8*, we generate a complete set of *bc8*-like phases with 16, 24, and 32 atoms per primitive cells and relax their structures *ab initio*.

BC8 STRUCTURE AND STRING SWITCHING

As it was mentioned in the Introduction, the atomic structure of the *bc8* phase can be considered as a set of atomic strings directed along threefold cubic axes (the

space group $Ia\bar{3}$, no. 206). Here the string structure is described in detail (Fig. 2). All the atoms are located at $16c$ sites x, x, x ($x = x_w \approx 0.1$) with threefold point symmetry and there are two nonequivalent inversion centers at $8a$ sites $0, 0, 0$ and $8b$ sites $\frac{1}{4}, \frac{1}{4}, \frac{1}{4}$. If we select one threefold axis, say $[111]$ passing through the origin $0, 0, 0$ (all threefold axes are equivalent), then its atoms have coordinates $(\frac{n}{2}, \frac{n}{2}, \frac{n}{2}) \pm (x_w, x_w, x_w)$, where n is an arbitrary integer. The A -bonds between neighboring atoms are $(2x_w, 2x_w, 2x_w)$ and they alternate with the next-neighbor distances A' along the threefold axis are $(\frac{1}{2} - 2x_w, \frac{1}{2} - 2x_w, \frac{1}{2} - 2x_w)$. Therefore the string of atoms looks like a sequence of alternating A -bonds (centered at inversion centers $\frac{n}{2}, \frac{n}{2}, \frac{n}{2}$) and 1.5 times longer stretches A' centered at inversion centers $\frac{1}{4} + \frac{n}{2}, \frac{1}{4} + \frac{n}{2}, \frac{1}{4} + \frac{n}{2}$ (Fig. 2b). The string of this type will be called *white*, hence the subindex w .

However, there is another value of x , $x = x_b = \frac{1}{4} - x_w$ which gives exactly the same $bc8$ structure rotated as a whole by the angle $\frac{\pi}{2}$ relative to the previous one (the subindex b means *black*). The black and white $bc8$ structures can be also transformed one to another by small local shifts of atoms along threefold directions resulting in rebonding of A -bonds, as has been suggested by Crain *et al.* [16] for the $r8$ phase and described above in the Introduction. In the string picture (Fig. 2c), the rebonding means simply that A' and A -bonds are locally permuted (switched), Fig. 2. Thus, for the black $bc8$, in the considered above $[111]$ string the A -bonds are centered at $\frac{1}{4} + \frac{n}{2}, \frac{1}{4} + \frac{n}{2}, \frac{1}{4} + \frac{n}{2}$ whereas A' at $\frac{n}{2}, \frac{n}{2}, \frac{n}{2}$.

An important observation is that any set of the strings can be independently switched from black to white without violation of energetically favorable tetrahedral coordination [23, 24]. The tetrahedral coordination means that each atom has four bonds with its neighbors, the lengths of bonds are not very different and all the interbond angles exceed $\frac{\pi}{2}$. An example of bond length and angle statistics can be found below. The switching of a single isolated string in the perfect $bc8$ phase has been simulated *ab initio* [24] and it has been found that it costs less than 0.02 eV per atom.

Obviously, if any string is allowed for switching independently of the others, then it is possible to obtain of about 2^N different structures, where the total number of strings N is proportional to the surface area of the crystal. This huge number of potential structures arises from a purely combinatorial consideration, without taking into account their relative energies. Note that all members of the infinite family of $bc8$ -like crystals have a close topological structure. Indeed, the string switching affects only one quarter of all bonds, namely, bonds lying along the axes (111) . Any similar phase can be obtained from $bc8$ by switching at most one eighth of the total number of bonds (Fig. 1).

Due to the black/white ambiguity, different switching combinations can define the same structure. For exam-

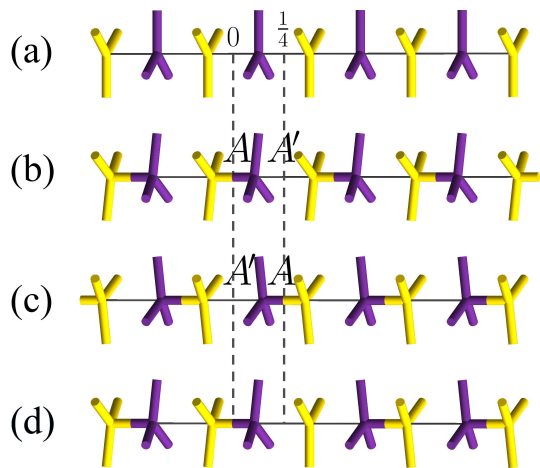


FIG. 2: (Color online) The mean position (a) and the white (b) and black (c) switching of an atomic string parallel to $[111]$ axis in the $bc8$ -like silicon. Shown are the A -bonds along the string, and the B -bonds with the atoms of other strings. The A -bonds are centered at points 0 (white) or $\frac{1}{4}$ (black) of the body diagonal of the cubic unit cell. When switching from white to black, the A -bonds are permuted with the A' -distances, and the atomic arrangement remains tetrahedral everywhere. In addition, the string can be split into white and black parts, separated by defects (d). The switching process may consist in moving such a defect along the string [35].

ple, two cases when all strings along the four cubic 3-fold axes have the same color, (w, w, w, w) or (b, b, b, b) , correspond to a single structure, namely $bc8$. Further, if the strings parallel to any two 3-fold axes are white, and those parallel to remaining two axes are black (the cases (w, w, b, b) , (w, b, w, b) , *etc.*), then the crystal symmetry become tetragonal and identical $bt8$ phases with different orientations of the tetragonal axis are obtained. Finally, if the sign of the strings parallel to any 3-fold axis is opposite to the sign of other strings, (w, w, w, b) , (w, b, b, b) , then identical $r8$ phases arise with different orientations of the rhombohedral axis. The three phases, $bc8$, $bt8$, and $r8$, exhaust the list of $bc8$ -like structures with the minimal primitive cell (8 atoms). Their common feature is that the parallel strings have the same color.

The fact that phases $bc8$ and $bt8$ are not connected by a group-subgroup relation suggests that there could be a more symmetrical structure which is parent to them both. For instance, it could be a structure with space group $Ia\bar{3}d$, which is a supergroup for both $Ia\bar{3}$ and $I4_1/a$. One evident way to construct the $Ia\bar{3}d$ structure is to turn all the strings into the half-switched state. In this case, all the atoms occupy $(16b)$ positions of $Ia\bar{3}d$ with three-coordinated graphite-like atomic environment (Fig. 2a). Atoms of each $Ia\bar{3}d$ string can be moved in one of two opposite directions until they reach positions with tetrahedral atomic environment (Fig. 2b or Fig. 2c). However, three-coordinated configurations are not favor-

able for silicon. Another, more physical way to obtain the $Ia\bar{3}d$ phase is to suppose that all the strings are randomly switched in one of the possible state black or white so that the $Ia\bar{3}d$ symmetry is a result of disorder [23]. In this case the transitions from $Ia\bar{3}d$ phase into $bc8$, $r8$, $bt8$, and more complicated superstructures could be of disorder-order type.

BC8-LIKE SUPERSTRUCTURES WITH ENLARGED PRIMITIVE CELLS

More complicated $bc8$ -like phases with larger primitive cells can occur, only when their parallel strings have different colors. The primitive cells of such phases are multiples in volume and number of atoms to the *primitive* cell of $bc8$ and the periods a, b, c of any cell are any three linearly independent periods of $bc8$. In addition, each cell constructed on arbitrarily selected periods of the initial bcc lattice can correspond to several phases with different space groups, depending on the colors of the strings passing through it. In order to enumerate and classify the structures, one need to calculate the number of independent, i.e. not connected by periodicity, strings in each of the four directions $\langle 111 \rangle$. To do this, the total length of the strings of the same direction, cut by the cell, should be divided by the smallest lattice period along the direction. For example, the number N_{111} of independent strings parallel to the axis $[111]$ of the group $Ia\bar{3}$ is equal to the greatest common divisor of three triple products

$$\begin{aligned} n_a &= (1, 1, 1) \cdot [\mathbf{b} \times \mathbf{c}], \\ n_b &= (1, 1, 1) \cdot [\mathbf{c} \times \mathbf{a}], \\ n_c &= (1, 1, 1) \cdot [\mathbf{a} \times \mathbf{b}], \end{aligned} \quad (1)$$

where \mathbf{a} , \mathbf{b} , and \mathbf{c} are the primitive cell periods, expressed in parameters of the initial bcc lattice.

The numbers $N_{\bar{1}\bar{1}\bar{1}}$, $N_{\bar{1}\bar{1}\bar{1}}$, and $N_{\bar{1}\bar{1}\bar{1}}$ can be calculated in the same way. The combinatorial amount of possible sets of independent string switching is equal to $2^{N_{111}+N_{\bar{1}\bar{1}\bar{1}}+N_{\bar{1}\bar{1}\bar{1}}+N_{\bar{1}\bar{1}\bar{1}}}$, however, the actual number of different phases is significantly less. For example, as mentioned above, in the case of the smallest primitive cell ($N_{111} = N_{\bar{1}\bar{1}\bar{1}} = N_{\bar{1}\bar{1}\bar{1}} = N_{\bar{1}\bar{1}\bar{1}} = 1$), 16 possible combinations of black/white switchings generate only 3 different phases, $bc8$, $bt8$, and $r8$. This significant reduction in the number of different structures is due to two reasons. First, some of the structures can be connected by the elements of the group $Ia\bar{3}d$, translations and rotations, not included in the their space group. Second, some combinations of switching can, in fact, correspond to smaller primitive cells.

Recently, several new silicon phases were experimentally observed with primitive cells two and four times larger than that of $bc8$ [30]. They are listed in the bottom part of Table I. Along with the names of these structures according to Ref. [30], we append the names in

accordance with our classification (in parentheses). In addition to conventional space groups of the crystals, the black and white (Shubnikov) groups are also presented. The last column shows three periods of the corresponding ideal unit cells, expressed in parameters of the initial bcc lattice of the $bc8$ phase. Indeed, all the phases listed in Table I, unlike some others (diamond, $st12$, etc.), belong to the same family and can be described in the language of string switching, Figs. 3–5.

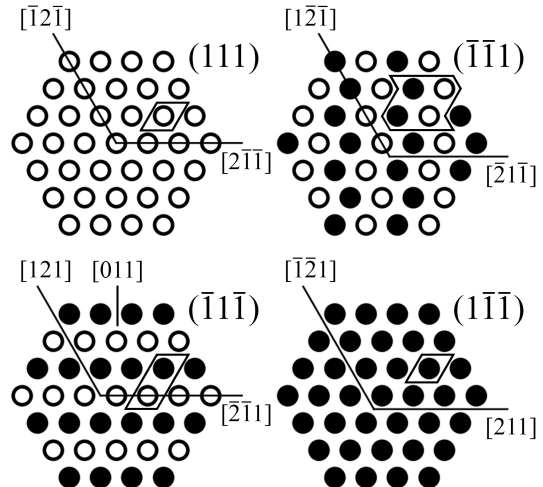


FIG. 3: Atomic strings in the $m32$ ($m32-8$) silicon phase in projections onto the planes $\{111\}$ perpendicular to them; white/black circles indicate white/black strings. For each projection its 2D generating cell is shown. For projections $\bar{1}\bar{1}\bar{1}$ and $\bar{1}\bar{1}\bar{1}$ the string switching alternates along the perpendicular directions $[011]$ and $[\bar{2}\bar{1}\bar{1}]$ correspondingly.

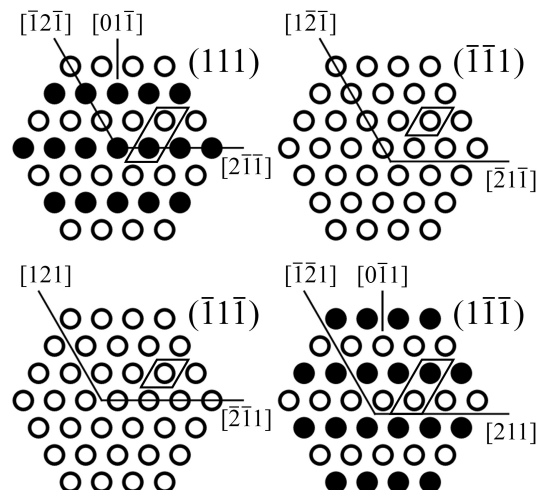


FIG. 4: Atomic strings in the $m32^*$ ($sm16-2$) silicon phase. The structure differs from the $bc8$ crystal by alternation of the string switching in two projections along the same direction $[01\bar{1}]$.

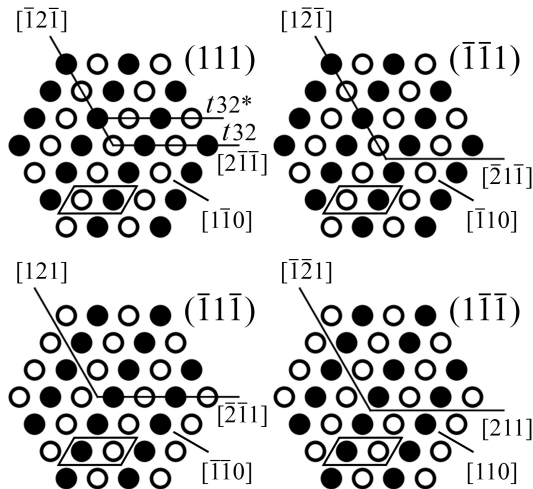


FIG. 5: Atomic strings in the $t32$ ($t32-1$) and $t32^*$ ($t32-3$) silicon phases. Both phases are characterized by alternation of the string switching along the perpendicular directions $[110]$ and $[\bar{1}\bar{1}0]$. The crystal $t32^*$ differs from $t32$ by the inverse switching of all the strings in one projection.

The list of structures in Table I is far from being exhaustive. As a first goal, we would like to find all the similar structures with double, triple and quadruple cells, i.e. containing 16, 24, and 32 silicon atoms in a primitive cell, respectively. The first step is to list all the different lattices with cells of the specified volumes with bases constructed from the vectors of the initial bcc lattice. Then, by switching independent strings passing through the cells, all possible structures can be found. In order to avoid double counting, the structures whose primitive cells turn out to have smaller volume should be discarded. For example, all structures with the basis vectors (100) , (010) , and (001) (lattice 16-2) actually have a primitive cell of the original bcc lattice and therefore they are exhausted by the previously listed phases $bc8$, $bt8$, and $r8$. Thus, it turns out that some lattices do not generate new phases. In other cases, different combinations of string switching can generate structures connected to each other by symmetry transformations. Such identical structures should also be discarded. The statistical results of the search are summarized in Table II. Seven lattices (one with double primitive cell, two with triple one, and four with quadruple one) give rise to 128 structures (or 177 if we consider the chiral enantiomorphs as different structures), four of which are listed in Table I. The Supplemental material contains the detailed description of atomic arrangements in those new phases, their energetic and structural relaxation (DFT simulations using QUANTUM ESPRESSO package [36, 37]) and attached crystallographic information files (CIFs) with atomic coordinates [38].

THE MAGNETIC ANALOGY

As can be seen on the example of the $bc8$, $bt8$, and $r8$ crystals, simultaneous switching of all strings of a crystal (hereinafter referred to as conjugation), e.g. from (w, w, w, w) to (b, b, b, b) , is equivalent to a rotation of the crystal as a whole and does not lead to the appearance of a new phase. The question arises whether this is a common property of such structures? The answer is no, and, indeed, already among the crystals with a double primitive cell, we find two different triclinic structures, $a16-3$ and $a16-4$, conjugated to each another. Note that this operation does not affect the elements of spatial symmetry and therefore both phases have the same space group. Nevertheless, their physical properties: energy, atomic density, cell parameters, etc., generally speaking, should differ.

In order to prove that conjugated structures have the same space group, an analogy with magnetic crystals can be suggested. Let us put in line with each silicon atom a displacement vector from the corresponding symmetric position $16b$ of the group $Ia\bar{3}d$ to its real position, in which it gets a fourth nearest neighbor. This vector is always parallel to the 3-fold axis passing through the atom, whereas its direction alternates along the axis. The situation resembles the ordering of magnetic moments arranged in the nodes of the original symmetric phase, provided that they are involved in two strong magnetic interactions: (i) a spin-orbit interaction, forcing the moments of individual atoms to align along the easy magnetization axes, which coincide with the 3-fold axes of the crystal; (ii) an antiferromagnetic exchange between neighboring atoms on the axes. Obviously, that in this analogy the operation of simultaneous switching of all strings plays the role of the time reversal operation. Thus, the lack of connection between the conjugation and the space group elements follows from the absence of such a connection for the time reversal operation. Note that the analogy is not complete, because, in contrast to the magnetic moment, the displacement of atom changes sign upon spatial inversion and does not change sign upon time inversion. As for the strings, it is easy to see that they change their color upon rotations of 90° and keep it unchanged for all other rotations of the cubic point group $m\bar{3}m$, as well as for the inversion. For example, the xyz -component of a magnetic octupole moment behaves in a similar way. The magnetic analogy allows one to enlarge the space group of a $bc8$ -like phase by adding symmetry elements transforming the structure into the conjugate one, and to describe the full symmetry by the use of Shubnikov magnetic groups [39–41]. If the magnetic group of a particular structure differs from its conventional space group, then this structure is self conjugate. Thus, the magnetic groups of the $bc8$, $bt8$ and $r8$ crystals are $Ia\bar{3}d'$, $I4_1/ac'd'$, and $R\bar{3}c'$, correspondingly (Table I). In Sup-

plemental material all the crystals are classified both by space and magnetic groups [38].

MICROSCOPIC STRUCTURE DETAILS

Let us analyze the distortions induced in the structure by the string switching. As has been mentioned in the Introduction, each atom has one A -bond parallel to a 3-fold axis and three non-symmetric B -bonds. In accordance with this fact two kind of angles between the bonds can be distinguished, the α angle between bonds A and B , and the β one between two B -bonds. The bonds tend to be of the same size. It is achieved, when the atoms are shifted along 3-fold axes by approximately $(\sqrt{3} - \sqrt{2})/8 \approx 0.0397$ lattice parameters from $16b$ positions of $Ia\bar{3}d$ group. Depending on the color of switching of neighboring strings, the angles α are subdivided into $\alpha' \approx 98.5^\circ$ and $\alpha'' \approx 94.3^\circ$, and the angles β into $\beta_1 \approx 107.0^\circ$, $\beta_2 \approx 117.9^\circ$, $\beta'_2 \approx 119.5^\circ$, and $\beta_3 \approx 130.6^\circ$ (Fig. 6). The statistical variation of the angles calculated from the structural data from [30] is shown in the graph using Gaussian distributions. It is seen that the angles α , β_1 , β_2 and β_3 are well distinguished. Apparently, the angles α close to 90° have the greatest energy disadvantage, and the microscopic structure undergoes additional distortion in order to increase them.

An important characteristic of a tetrahedral structure is the statistics of atomic rings. All considered $bc8$ -like phases have the girth (i.e. minimal ring) equal to five, except for the $bc8$ itself, made up exclusively of six-membered rings. For the first approximation, we can investigate the dependence of the physical properties of the crystals on the number of five-membered rings per atom, which varies from $\nu_5 = 0$ for $bc8$ to $\nu_5 = 1$ for $bt8$. Fig. 7 shows dependencies of the energy and volume per atom on ν_5 calculated for several $bc8$ -like phases. It follows from the figure that with increasing frequency of five-membered rings the tendency is observed to increase in energy and decrease in the volume of the crystal.

The number of five-membered rings in a $bc8$ -like phase correlates with the frequencies of different angles from Fig. 6. The five-membered rings appear only upon the string switching, when bonds are formed between black and white strings. Moreover, a necessary and sufficient condition for making a five-membered ring is the local configuration containing the angle β_1 at an atom. Thus, the number of five-membered rings coincides with the number of the β_1 angles. In addition to the vertex with the angle β_1 , each five-membered ring has a vertex α' and three vertices α'' . Besides, an α'' angle can be common for two adjacent five-membered rings. Using relations between the numbers of angles of different type in $bc8$ -like structures, we find that $\nu_{\alpha'} = 3 - 2\nu_5$, $\nu_{\alpha''} = 2\nu_5$, $\nu_{\beta_1} = \nu_{\beta'_2} = \nu_{\beta_3} = \nu_5$, $\nu_{\beta_2} = 3 - 3\nu_5$.

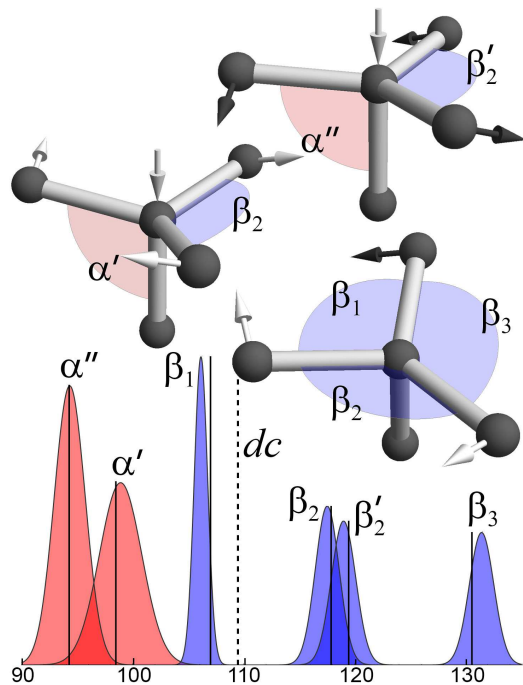


FIG. 6: (Color online) The angles between interatomic bonds in the $bc8$ -like structures depending on the white/black color of switching of adjacent strings. The α angles are between bonds A and B , and the β ones are between B -bonds. In the plot, the Gaussians approximate statistical data on real $bc8$ -like crystals from Ref. [30]. The vertical lines correspond to ideal displacements of atoms by $(\sqrt{3} - \sqrt{2})/8 \approx 0.0397$ lattice parameters from the average $16b$ positions of $Ia\bar{3}d$ group. The dashed line corresponds to the angle between the bonds in the diamond crystal, $\arccos(-1/3) \approx 109.5^\circ$.

DISCUSSION AND CONCLUSIONS

In summary, we described in detail the physical mechanism behind the complicated silicon structures observed by Rapp *et al.* after ultrashort laser microexplosions [30]. Those silicon phases (except $st12$) can be obtained from the $bc8$ phase by switching the $\langle 111 \rangle$ atomic strings in different regular (periodic) ways. The stochastic switching of the strings gives a disordered phase with $Ia\bar{3}d$ cubic symmetry, and the space groups of the $bc8$ -like phases are subgroups of $Ia\bar{3}d$. All the possible phase transitions between different $bc8$ -like phases should be of the first order (not continuous) because atoms of the switched strings jump over finite distances.

Our consideration suggests a possible scenario for the observed polymorphism of $bc8$ -like phases. It was shown in Ref. [24], that the reduced intensity functions (the structure-dependent parts of the X-ray scattering pattern), are very similar for amorphous silicon and for disordered polycrystalline $Ia\bar{3}d$ phase. Thus, we can suppose that the high-temperature/high-pressure amorphous phase first transforms into disordered $Ia\bar{3}d$ phase

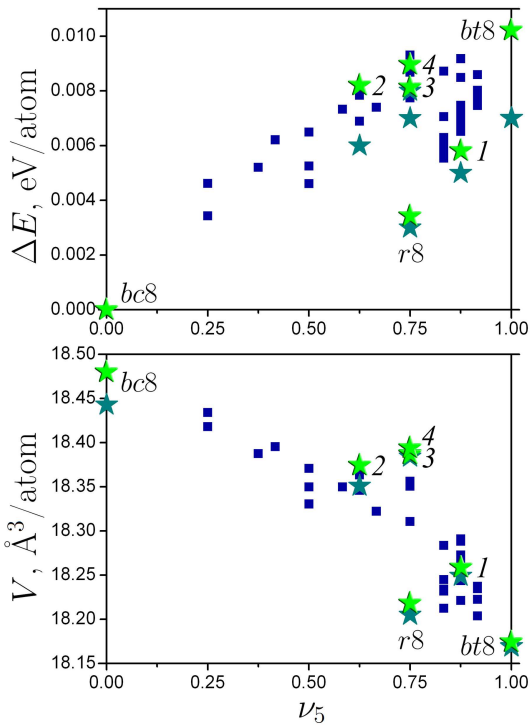


FIG. 7: (Color online) The energy and the volume per atom for *bc8*-like structures depending on the frequency ν_5 of five-membered rings calculated *ab initio*; the stars indicate experimentally observed structures, green for our results and dark cyan for the data from Ref. [30]: 1 — *m32* (*m32-8*), 2 — *m32** (*sm16-2*), 3 — *t32* (*t32-1*), 4 — *t32** (*t32-3*); the squares are for some new structures described in the present paper. The energy is measured from that of *bc8*.

and then, depending on local temperature, pressure, and shear, into different *bc8*-like phases for which *Ia3d* is the parent phase. It would be important to study carefully the diffraction patterns of experimentally observed phases because of predicted rich polymorphism of *bc8*-like phases.

It would be very interesting to use the technique of Rapp et al. [30] for the *bc8* crystals instead of diamond silicon because in this case new *bc8*-type phases will grow inside the parent *bc8* matrix. Reasonably large phase-pure *bc8* polycrystals (several mm size) have been grown recently by different methods [42, 43].

Acknowledgements

We are grateful to S. A. Pikin, S. M. Stishov, M. V. Gorkunov, M. Kléman, and C. J. Pickard for useful discussions and communications. This work was supported by the Ministry of Science and Higher Education of the Russian Federation within the State assignment FSRC “Crystallography and Photonics” RAS in part of symmetry analysis, and by the grant of Prezidium of

Russian Academy of Sciences in part of computer simulations.

-
- [1] J. Crain, G. J. Ackland, and S. J. Clark, Exotic structures of tetrahedral semiconductors. *Rep. Prog. Phys.* **58**, 705-54 (1995).
 - [2] Q. Fan, C. Chai, Q. Wei, H. Yan, Y. Zhao, Y. Yang, X. Yu, Y. Liu, M. Xing, J. Zhang, and R. Yao, Novel silicon allotropes: Stability, mechanical, and electronic properties. *J. Appl. Phys.* **118**, 185704 (2015).
 - [3] G. J. Ackland, High-pressure phases of group IV and III-V semiconductors. *Rep. Prog. Phys.* **64**, 483-516 (2001).
 - [4] A. Mujica, A. Rubio, A. Muñoz, and R. J. Needs, High-pressure phases of group-IV, III-V, and II-VI compounds. *Rev. Mod. Phys.* **75**, 863-912 (2003).
 - [5] B. Haberl, T. A. Strobel, and J. E. Bradby, Pathways to exotic metastable silicon allotropes. *Appl. Phys. Rev.* **3**, 040808 (2016).
 - [6] M. Tilli, T. Motooka, V.-M. Airaksinen, S. Franssila, M. Paulasto-Kröckel, and V. Lindroos (eds.), *Handbook of Silicon Based MEMS Materials and Technologies - 2nd Edition* (Elsevier, 2015).
 - [7] R. H. Wentorf, Jr. and J. S. Kasper, Two new forms of silicon. *Science* **139**, 338-9 (1963).
 - [8] J. S. Kasper and S. M. Richards, The crystal structures of new forms of silicon and germanium. *Acta Cryst.* **17**, 752-5 (1964).
 - [9] J. D. Joannopoulos and M. L. Cohen, Electronic properties of complex crystalline and amorphous phases of Ge and Si. I. Density of states and band structures. *Phys. Rev. B* **7**, 2644-57 (1973).
 - [10] J. D. Joannopoulos and M. L. Cohen, Electronic properties of complex crystalline and amorphous phases of Ge and Si. II. Band structure and optical properties. *Phys. Rev. B* **8**, 2733-55 (1973).
 - [11] M. T. Yin, Si-III (BC-8) crystal phase of Si and C: Structural properties, phase stabilities, and phase transitions. *Phys. Rev. B* **30**, 1773-6 (1984).
 - [12] R. Biswas, R. M. Martin, R. J. Needs, and O. H. Nielsen, Stability and electronic properties of complex structures of silicon and carbon under pressure: Density-functional calculations. *Phys. Rev. B* **35**, 9559-68 (1987).
 - [13] J. Crain, S. J. Clark, G. J. Ackland, M. C. Payne, V. Milman, P. D. Hatton, and B. J. Reid, Theoretical study of high-density phases of covalent semiconductors. I. *Ab initio* treatment. *Phys. Rev. B* **49**, 5329-40 (1994).
 - [14] S. J. Clark, G. J. Ackland, and J. Crain, Theoretical study of high-density phases of covalent semiconductors. II. Empirical treatment. *Phys. Rev. B* **49**, 5341-52 (1994).
 - [15] H. Zhang, H. Liu, K. Wei, O. O. Kurakevych, Y. Le Godec, Z. Liu, J. Martin, M. Guerrette, G. S. Nolas, and T. A. Strobel, BC8 silicon (Si-III) is a narrow-gap semiconductor. *Phys. Rev. Lett.* **118**, 146601 (2017).
 - [16] J. Crain, G. J. Ackland, J. R. Maclean, R. O. Piltz, P. D. Hatton, and G. S. Pawley, Reversible pressure-induced structural transitions between metastable phases of silicon. *Phys. Rev. B* **50**, 13043-46 (1994).
 - [17] S. V. Demishev, D. G. Lunts, D. V. Nekhaev, N. E. Sluchanko, N. A. Samarin, V. V. Brazhkin, A. G. Lyapin, S. V. Popova, and N. N. Mel'nik, Structural relaxation of

- the metastable Kasper phase of silicon. *JETP* **82**, 1159 (1996).
- [18] V. Domnich and Y. Gogotsi, Phase transformations in silicon under contact loading. *Rev. Adv. Mater. Sci.* **3**, 1-36 (2002).
- [19] B. Haberl, M. Guthrie, S. V. Sinogeikin, G. Shen, J. S. Williams, and J. E. Bradby, Thermal evolution of the metastable r8 and bc8 polymorphs of silicon. *High Pressure Research.* **35**, 99-116 (2015).
- [20] S. Wong, B. C. Johnson, B. Haberl, A. Mujica, J. C. McCallum, J. S. Williams, and J. E. Bradby, Thermal evolution of the indentation-induced phases of silicon. *J. Appl. Phys.* **126**, 105901 (2019).
- [21] B. D. Malone, J. D. Sau, and M. L. Cohen, Ab initio study of the optical properties of Si-XII, *Phys. Rev. B* **78**, 161202 (2008).
- [22] S. Wong, B. Haberl, B. C. Johnson, A. Mujica, M. Guthrie, J. C. McCallum, J. S. Williams, and J. E. Bradby, Formation of an r8-dominant Si material, *Phys. Rev. Lett.* **122**, 105701 (2019).
- [23] V. E. Dmitrienko and M. Kléman, Icosahedral order and disorder in semiconductors. *Phil. Mag. Lett.* **79**, 359-67 (1999).
- [24] V. E. Dmitrienko, M. Kléman, and F. Mauri, Quasicrystal-related phases in tetrahedral semiconductors: Structure, disorder, and ab initio calculations. *Phys. Rev. B* **60**, 9383-9 (1999).
- [25] V. E. Dmitrienko, M. Kléman, and F. Mauri, Silicon and carbon structures with icosahedral order, phason jumps, and disorder. *Ferroelectrics* **250**, 213-218 (2001).
- [26] J.-T. Wang, C. F. Chen, H. Mizuseki, and Y. Kawazoe, Kinetic origin of divergent decompression pathways in silicon and germanium. *Phys. Rev. Lett.* **110**, 165503 (2013).
- [27] T. Ishikawa, N. Suzuki, and K. Shimizu, Crystal structure searching by free energy surface trekking: application to carbon at 1 TPa. *J. Phys.: Conf. Ser.* **500**, 162003 (2014).
- [28] V. S. Kraposhin, A. L. Talis, V. G. Kosushkin, A. A. Ogneva, and L. I. Zinober, Structures of the cubic and rhombohedral high-pressure modifications of silicon as packing of the rod-like substructures determined by the algebraic geometry. *Acta Cryst. B* **64**, 26-33 (2008).
- [29] V. E. Dmitrienko and M. Kléman, Icosahedral order and disorder in tetrahedral semiconductors. Three-dimensional and six-dimensional views. *Mater. Sci. Eng.* **294-296**, 246-9 (2000).
- [30] L. Rapp, B. Haberl, C. J. Pickard, J. E. Bradby, E. G. Gamaly, J. S. Williams, and A. V. Rode, Experimental evidence of new tetragonal polymorphs of silicon formed through ultrafast laser-induced confined microexplosion. *Nat. Commun.* **6**, 7555 (2015).
- [31] L. Rapp, B. Haberl, J. E. Bradby, E. G. Gamaly, J. S. Williams, and A. V. Rode, Confined micro-explosion induced by ultrashort laser pulse at SiO₂/Si interface. *Appl. Phys. A* **114**, 33-43 (2014).
- [32] A. Mujica, C. J. Pickard, and R. J. Needs, Low-energy tetrahedral polymorphs of carbon, silicon, and germanium. *Phys. Rev. B* **91**, 214104 (2015).
- [33] Q. Zhu, A. R. Oganov, A. O. Lyakhov, and X. Yu, Generalized evolutionary metadynamics for sampling the energy landscapes and its applications. *Phys. Rev. B* **92**, 024106 (2015).
- [34] S. Ruffell, J. VEDI, J. E. Bradby, and J. S. Williams, Effect of hydrogen on nanoindentation-induced phase transformations in amorphous silicon, *J. Appl. Phys.* **106**, 123511 (2009).
- [35] See Supplemental Material at [URL] for the animated image of the string switching process.
- [36] QUANTUM ESPRESSO, <http://www.quantum-espresso.org/>
- [37] P. Giannozzi, S. Baroni, N. Bonini, M. Calandra, R. Car, C. Cavazzoni, D. Ceresoli, G. L. Chiarotti, M. Cococcioni, I. Dabo, A. Dal Corso, S. de Gironcoli, S. Fabris, G. Fratesi, R. Gebauer, U. Gerstmann, C. Gougousis, A. Kokalj, M. Lazzeri, L. Martin-Samos, N. Marzari, F. Mauri, R. Mazzarello, S. Paolini, A. Pasquarello, L. Paulatto, C. Sbraccia, S. Scandolo, G. Sclauzero, A. P. Seitsonen, A. Smogunov, P. Umari, and R. M. Wentzcovitch, QUANTUM ESPRESSO: a modular and open-source software project for quantum simulations of materials. *J. Phys.: Condens. Matter* **21**, 395502 (2009).
- [38] See Supplemental Material at [URL] for the description of new bc8-like phases with enlarged primitive cells and corresponding crystallographic information files (CIF).
- [39] D. B. Litvin, *Magnetic group tables: 1-, 2-, and 3-dimensional magnetic superperiodic groups and magnetic space groups* (International Union of Crystallography, 2013).
- [40] Bilbao Crystallographic Server, <http://www.cryst.ehu.es/>
- [41] J. M. Perez-Mato, S. V. Gallego, E. S. Tasci, L. Elcoro, G. de la Flor, and M. I. Aroyo, Symmetry-based computational tools for magnetic crystallography. *Annu. Rev. Mater. Res.* **45**, 217 (2015).
- [42] O. O. Kurakevych, Y. Le Godec, W. A. Crichton, J. Guignard, T. A. Strobel, H. Zhang, H. Liu, C. Coelho Diogo, A. Polian, N. Menguy, S. J. Juhl, and C. Gervais, Synthesis of bulk BC8 silicon allotrope by direct transformation and reduced-pressure chemical pathways. *Inorg. Chem.*, **55**, 8943-8950 (2016).
- [43] X. Li, Z. Li, K. Yang, and D. He, Phase-pure bulk BC8 silicon prepared through secondary phase transition method under high pressure, *Materials Lett.* (2019), doi: <https://doi.org/10.1016/j.matlet.2019.127195>

TABLE I: Known $bc8$ -like silicon phases

phase	Fedorov group	Shubnikov group	unit cell ideal periods
$bc8$	$Ia3$ (206)	$Ia3d'$ (230.148)	} (100), (010), (001)
$bt8$	$I4_1/a$ (88)	$I4_1/ac'd'$ (142.567)	
$r8$	$R\bar{3}$ (148)	$R\bar{3}c'$ (167.107)	$(\frac{1}{2}\frac{1}{2}\frac{1}{2})$, $(\frac{1}{2}\frac{1}{2}\bar{1})$, $(\frac{1}{2}\bar{1}\frac{1}{2})$
$m32$ ($m32-8$)	$P2_1/c$ (14)	$P2_1/c$ (14.75)	$(\frac{1}{2}\frac{1}{2}\frac{1}{2})$, (011), $(\frac{3}{2}\frac{1}{2}\frac{1}{2})$
$m32^*$ ($sm16-2$)	$C2$ (5)	$C22'2'$ (21.41)	(100), (011), (011)
$t32$ ($t32-1$)	$P\bar{4}2_1c$ (114)	$P_C\bar{4}2_1c$ (114.281)	} (110), (110), (001)
$t32^*$ ($t32-3$)	$P4_32_12$ (96)	$P_C4_32_12$ (96.149)	

TABLE II: The supercells multiple to the primitive cell of $bc8$ and the numbers of generated $bc8$ -like structures

cell names	ideal periods (in periods of the primitive $bc8$ cell)	multiplicity	number of structures without/with enantiomorphs	known structures
8-1	$(\frac{1}{2}, \frac{1}{2}, \frac{1}{2})$, $(\frac{1}{2}, \frac{1}{2}, \bar{1})$, $(\frac{1}{2}, \bar{1}, \frac{1}{2})$	1	3/3	$bc8$, $r8$, $bt8$
16-1	$(\frac{1}{2}, \frac{1}{2}, \frac{1}{2})$, $(\frac{1}{2}, \frac{1}{2}, \bar{1})$, (1, 0, $\bar{1}$)	2	6/8	$m32^*$
16-2	(1, 0, 0), (0, 1, 0), (0, 0, 1)	2	—	
24-1	$(\frac{1}{2}, \frac{1}{2}, \frac{1}{2})$, $(\frac{1}{2}, \frac{1}{2}, \bar{1})$, $(\frac{3}{2}, \frac{1}{2}, \frac{3}{2})$	3	18/23	
24-2	$(\frac{1}{2}, \frac{1}{2}, \frac{1}{2})$, (0, $\bar{1}$, 1), (1, 0, $\bar{1}$)	3	4/4	
24-3	(1, 0, 0), (0, 1, 0), $(\frac{1}{2}, \frac{1}{2}, \frac{3}{2})$	3	—	
32-1	(1, 0, 0), (0, 1, 1), (0, $\bar{1}$, 1)	4	6/8	
32-2	$(\frac{1}{2}, \frac{1}{2}, \frac{1}{2})$, $(\frac{1}{2}, \frac{1}{2}, \bar{1})$, (2, 0, $\bar{2}$)	4	46/68	$m32$
32-3	$(\frac{1}{2}, \frac{1}{2}, \frac{1}{2})$, (1, 0, $\bar{1}$), $(\frac{1}{2}, \frac{3}{2}, \frac{1}{2})$	4	22/26	
32-4	$(\frac{3}{2}, \frac{1}{2}, \frac{1}{2})$, $(\frac{1}{2}, \frac{3}{2}, \frac{1}{2})$, $(\frac{1}{2}, \frac{1}{2}, \frac{3}{2})$	4	26/40	
32-5	(1, 0, 0), (0, $\bar{1}$, 0), (0, 0, 2)	4	—	
32-6	(1, 0, 1), (0, 1, 1), (0, $\bar{1}$, 1)	4	—	
32-7	(1, 0, 1), (1, 1, 0), (0, 1, 1)	4	—	
32-8	(1, 0, $\bar{1}$), (0, 1, 0), $(\frac{1}{2}, \frac{1}{2}, \frac{3}{2})$	4	—	
			Total: 131/180	

SUPPLEMENTAL MATERIAL

Animated GIFs

Animation *bondon.gif* demonstrates a probable mechanism of the string switching from white to black and back. The process involves moving a dangling interatomic bond along a 3-fold axis, which can be associated with a quasi-particle called “bondon”. Note that the sign of switching does not correlate with the direction of bondon movement.

Crystallographic information files

For generation and enumeration of possible *bc8*-like phases we use an approach based on the “ideal” atomic structure of the *bc8* phase as a crystalline approximant of icosahedral quasicrystals where the switches of the string correspond to phasonic jumps of atoms [23, 25, 29]. In this case, the *A* and *B* interatomic bonds are parallel, correspondingly, to three- and fivefold axes of an icosahedron, with the ratio of bonds $r_B/r_A = \sqrt{(\tau + 2)}/3 \approx 1.098$ ($\tau = (1 + \sqrt{5})/2$ is the golden mean). When the string is switched, the *A* bonds remains of the same length and the third type of bonds (*C*-bonds) appears, connecting atoms at switched and non-switched strings.

The folder *cifs_.zip* contains Crystallographic Information Files (CIFs) with atomic coordinates in such ideal representation. The cell parameters are calculated based on the ideal *bc8* crystal period $a = 6.658\text{\AA}$. Note that the crystal lattices of the idealized structures are characterized by the unit cell parameters (angles, ratio of periods) characteristic of the cubic lattice of the *bc8* phase. A real structure may have slightly distorted cell parameters if phase symmetry allows it. The files from the folder *cifs_.zip* describe the structures as having the least symmetrical group *P1*. All positions are listed for the primitive cell. Some of the structures have been relaxed using *ab initio* simulations. In these cases, the cif-file, tagged by an extra underscore symbol, also contains the refined crystallographic data. The *cifs_.zip* file can be sent by request.

Details of ab initio simulation

For the *ab initio* DFT relaxation of the initial “ideal” *bc8*-like structures we used the QUANTUM ESPRESSO code [36, 37]. We selected the generalized gradient approximation (GGA) with the Perdew–Burke–Ernzerhof (PBE) exchange-correlation functional which seems to provide better agreement between experimental and theoretical lattice parameters than the local density approximation (LDA). We used the ultra-soft pseudopotential *Si.pbe-n-rrkjus_psl.1.0.0.UPF* [36], the plane-wave energy

cutoff of 40 Ry, and the structural relaxations were supposed to be converged when all of the interatomic forces were less than 10^{-3} Ry/a.u. The *bc8*-like structures relaxed this way are presented in the cif-files tagged by an extra underscore symbol in the file names. This includes all *bc8*-like structures with the lattices 16-1, 24-1, 24-2, 32-1, the monoclinic phases *m32*-6,7,8 with the lattice 32-3, and the rhombohedral phases *r32*-3,4,5,6 with the lattice 32-4.

Lattices and structures

Below 131 *bc8*-like phases are listed and classified (180 with chiral enantiomorphs). The list exhausts all similar structures with 8, 16, 24, and 32 atoms in primitive cells, including previously known ones (*bc8*, *bt8*, *r8*, *m32*-8 (*m32* [30]), *sm16*-2 (*m32** [30]), *t32*-1 (*t32* [30]), *t32*-3 (*t32** [30])), and 124 structures proposed for the first time.

The description of structures corresponds to the following scheme.

Lattice type. The phases described are divided into eight different lattices: one each with 8 and 16 atoms in primitive cell, two with 24 atoms, and four with 32 atoms. Every lattice is defined by periods, which coincides with some periods of the *bcc* lattice of the *bc8* crystal. The type of Bravais lattice is indicated.

Symmetry. The structures of *bc8*-like phases are classified by their symmetry. Crystals with the same symmetry are combined together. Listed are the space groups, the Pearson symbols, and the black-white magnetic groups (in red) of the structures.

Structures. The name of each phase is constructed according to the *csN-n* scheme, where the optional symbol *c* means centering (*b*: body-centered, *s*: base-centered), *s* indicates crystal system (*a*: triclinic, *m*: monoclinic, *t*: tetragonal, *r*: rhombohedral, *h*: hexagonal, *c*: cubic), *N* is the number of atoms in the primitive cell, *n* is the sequence number. For a chiral structure, its enantiomorph is indicated in parentheses.

LATTICE 8

PERIODS: $a(\frac{1}{2}, \frac{1}{2}, \frac{1}{2})$, $a(\frac{1}{2}, \frac{1}{2}, \frac{1}{2})$, $a(\frac{1}{2}, \frac{1}{2}, \frac{1}{2})$

BRAVAIS LATTICE: body-centered cubic

STRUCTURES:

$Ia\bar{3}$ (206); $cI16$; $Ia\bar{3}d'$ (230.148) : *bc8*

$I4_1/a$ (88); $tI16$; $I4_1/ac'd'$ (142.567) : *bt8*

$R\bar{3}$ (148); $hR24$; $R\bar{3}c'$ (167.107) : *r8*

LATTICE 16-1PERIODS: $a(\frac{1}{2}, \frac{1}{2}, \frac{1}{2}), a(\frac{1}{2}, \frac{1}{2}, \bar{1}), a(1, 0, \bar{1})$

BRAVAIS LATTICE: base-centered orthorhombic

STRUCTURES:

 $C2$ (5); $mC32$; $C2'2'2'$ (21.41) : $sm16-1(2)$ $P2_1$ (4); $mP16$; $C2'2'2_1$ (20.33) : $m16-1(2)$ $P\bar{1}$ (2); $aP16$; $P2'/c'$ (13.69) : $a16-1, a16-2$ $P\bar{1}$ (2.4) : $a16-3, a16-4$ **LATTICE 24-1**PERIODS: $a(\frac{1}{2}, \frac{1}{2}, \frac{1}{2}), a(\frac{1}{2}, \frac{1}{2}, \bar{1}), a(\frac{3}{2}, \frac{1}{2}, \frac{3}{2})$

BRAVAIS LATTICE: face-centered orthorhombic

STRUCTURES:

 $C2/c$ (15); $mC48$; $Fd'd'd$ (70.530) : $sm24-1, sm24-2$ $C2$ (5); $mC48$; $F2'2'2$ (22.47) : $sm24-3(5), sm24-4(6)$ $P\bar{1}$ (2); $aP24$; $C2'/c'$ (15.89) : $a24-1, a24-2, a24-3, a24-4, a24-5$ $C2'/c'$ (15.89) : $a24-6, a24-7$ $P\bar{1}$ (2.4) : $a24-8, a24-9, a24-10, a24-11$ $P1$ (1); $aP24$; $C2'$ (5.15) : $a24-12(13), a24-14(15), a24-16(17)$ **LATTICE 24-2**PERIODS: $a(\frac{1}{2}, \frac{1}{2}, \frac{1}{2}), a(0, \bar{1}, 1), a(1, 0, \bar{1})$

BRAVAIS LATTICE: hexagonal

STRUCTURES:

 $P\bar{3}$ (147); $hP24$; $P\bar{3}c'1$ (165.95) : $h24-1, h24-2$ $P\bar{1}$ (2); $aP24$: $C2'/c'$ (15.89) : $a24-18, a24-19$ **LATTICE 32-1**PERIODS: $a(1, 0, 0), a(0, 1, 1), a(0, \bar{1}, 1)$

BRAVAIS LATTICE: tetragonal

STRUCTURES:

 $P\bar{4}2_1c$ (114); $tP32$; $P\bar{C}4_2c$ (114.281) : $t32-1$ $P4_12_12$ (92); $tP32$; $P_C4_12_12$ (92.117) : $t32-2(3)$ $P4_32_12$ (96); $tP32$; $P_C4_32_12$ (96.149) : $t32-3(2)$ $C2/c$ (15); $mC64$; $C2/c$ (15.85) : $sm32-1, sm32-2$ $P\bar{1}$ (2); $aP32$; $C2'/c'$ (15.89) : $a32-1$ $P1$ (1); $aP32$; $P2'$ (3.3) : $a32-2(3)$ **LATTICE 32-2**PERIODS: $a(\frac{1}{2}, \frac{1}{2}, \frac{1}{2}), a(\frac{1}{2}, \frac{1}{2}, \bar{1}), a(2, 0, \bar{2})$

BRAVAIS LATTICE: base-centered orthorhombic

STRUCTURES:

 $C2$ (5); $mC64$; $C2'2'2'$ (21.41) : $sm32-3(9), sm32-4(10), sm32-5(11), sm32-6(12), sm32-7(13), sm32-8(14)$ $P2_1$ (4); $mP32$; $C2'2'2_1$ (20.33) : $m32-1(3), m32-2(4)$ $P\bar{1}$ (2); $aP32$; $P2'/c'$ (13.69) : $a32-4, a32-5, a32-6, a32-7, a32-8, a32-9, a32-10, a32-11, a32-12, a32-13, a32-14, a32-15$ $P\bar{1}$ (2.4) : $a32-16, a32-17, a32-18, a32-19, a32-20, a32-21, a32-22, a32-23, a32-24, a32-25, a32-26, a32-27$ $P1$ (1); $aP32$; $C2'$ (5.15) : $a32-28(30), a32-29(31), a32-32(34), a32-33(35)$ $P2'$ (3.3) : $a32-36(42), a32-37(43), a32-38(44), a32-39(45), a32-40(46), a32-41(47)$ $P1$ (1.1) : $a32-48(52), a32-49(53), a32-50(54), a32-51(55)$ **LATTICE 32-3**PERIODS: $a(\frac{1}{2}, \frac{1}{2}, \frac{1}{2}), a(1, 0, \bar{1}), a(\frac{1}{2}, \frac{3}{2}, \bar{1})$

BRAVAIS LATTICE: monoclinic

STRUCTURES:

 $P2_1/c$ (14); $mP32$; $P2_1/c$ (14.75) : $m32-5, m32-6, m32-7, m32-8$ $P\bar{1}$ (2); $aP32$; $P2'/c'$ (13.69) : $a32-56, a32-57, a32-58, a32-59$ $P2'_1/c'$ (14.79) : $a32-60, a32-61$ $P\bar{1}$ (2.4) : $a32-62, a32-63, a32-64, a32-65, a32-66, a32-67, a32-68, a32-69$ $P1$ (1); $aP32$; $P2'$ (3.3) : $a32-70(72), a32-71(73)$ $P1$ (1.1) : $a32-74(76), a32-75(77)$ **LATTICE 32-4**PERIODS: $a(\frac{3}{2}, \frac{1}{2}, \bar{1}), a(\frac{1}{2}, \frac{3}{2}, \bar{1}), a(\frac{1}{2}, \frac{1}{2}, \frac{3}{2})$

BRAVAIS LATTICE: rhombohedral

STRUCTURES:

 $R\bar{3}$ (148); $hR96$; $R\bar{3}c'$ (167.107) : $r32-1, r32-2$

$R3$ (146); $hR96$; $R32'$ (155.47) : $r32-3(5)$, $r32-4(6)$

$P\bar{1}$ (2); $aP32$;

$C2'/c'$ (15.89) : $a32-78$, $a32-79$, $a32-80$, $a32-81$, $a32-82$, $a32-83$

$P\bar{1}$ (2.4) : $a32-84$, $a32-85$, $a32-86$, $a32-87$

$P1$ (1); $aP32$

Cc' (9.39) : $a32-88(90)$, $a32-89(91)$

$C2'$ (5.15) : $a32-92(98)$, $a32-93(99)$, $a32-94(100)$, $a32-95(101)$, $a32-96(102)$, $a32-97(103)$

$P1$ (1.1) : $a32-104(108)$, $a32-105(109)$, $a32-106(110)$, $a32-107(111)$